# Dissociative Changes in the $B_{max}$ and $K_D$ of Dopamine $D_2/D_3$ Receptors with Aging Observed in Functional Subdivisions of the Striatum: A Revisit with an Improved Data Analysis Method

Hiroto Kuwabara[1], Mary E. McCaul[2,3], Gary S. Wand[2,3], Christopher J. Earley[4], Richard P. Allen[4], Elise M. Weerts[2], Robert F. Dannals[1], and Dean F. Wong[1,2,5]

*[1]Department of Radiology, Johns Hopkins University School of Medicine, Baltimore, Maryland; [2]Department of Psychiatry and Behavioral Sciences, Johns Hopkins University School of Medicine, Baltimore, Maryland; [3]Department of Medicine, Johns Hopkins University School of Medicine, Baltimore, Maryland; [4]Department of Neurology, Johns Hopkins University School of Medicine, Baltimore, Maryland; and [5]Department of Neuroscience; Johns Hopkins University School of Medicine, Baltimore, Maryland*

Separate measurements of $B_{max}$, the density of available receptors, and $K_D$, the equilibrium dissociation constant in the human brain, with PET have contributed to our understanding of neuropsychiatric disorders, especially with respect to the dopamine $D_2/D_3$ receptor system. However, existing methods have limited applications to the whole striatum, putamen, or caudate nucleus. Improved methods are required to examine $B_{max}$ and $K_D$ in detailed functional striatal subdivisions that are becoming widely used. **Methods:** In response, a new method (bolus-plus-infusion transformation [BPIT]) was developed. After completion of a validation study for $^{11}$C-raclopride scans involving 81 subjects, age-associated changes in $B_{max}$ and $K_D$ were examined in 47 healthy subjects ranging in age from 18 to 77 y. **Results:** The BPIT method was consistent with established reference tissue methods regarding regional binding potential. BPIT yielded time-consistent estimates of $B_{max}$ and $K_D$ when scan and infusion lengths were set equal in the analysis. In addition, BPIT was shown to be robust against PET measurement errors when compared with a widely accepted transient equilibrium method. Altogether, BPIT was supported as a method for regional binding potential, $B_{max}$, and $K_D$. We demonstrated age-associated declines in $B_{max}$ in all 5 functional striatal subdivisions with BPIT when corrected for multiple comparisons. These age-related effects were not consistently attainable with the transient equilibrium method. Irrespective to methods, $K_D$ remained unchanged with age. **Conclusion:** The BPIT approach may be useful for understanding dopamine receptor abnormalities in neuropsychiatric disorders by enabling separate measurements of $B_{max}$ and $K_D$ in functional striatal subdivisions.

**Key Words:** receptor density; dopamine $D_2/D_3$ receptors; aging; functional striatal subdivisions; $^{11}$C-raclopride

**J Nucl Med 2012; 53:805–812**
DOI: 10.2967/jnumed.111.098186

Received Sep. 12, 2011; revision accepted Jan. 3, 2012.
For correspondence or reprints contact: Hiroto Kuwabara, 601 N. Caroline St., JHOC Room 3230, Baltimore, MD 21287.
E-mail: hkuwaba1@jhmi.edu
Published online Apr. 9, 2012.


Measurements of $B_{max}$, the density of available receptors, and $K_D$, the equilibrium dissociation constant in humans, with PET have contributed to our understanding of neuropsychiatric disorders, in particular on the role of dopamine $D_2/D_3$ receptors in schizophrenia (*1–3*). From the methodologic standpoint, the transient equilibrium method (TEM) (as referred to by Hietala et al. (*4*)) that was advanced by Farde et al. (*5*) is of particular significance, being widely used with the reversible radioligand $^{11}$C-raclopride. TEM, using the cerebellum as the reference region, yielded $B_{max}$ and $K_D$ values in the putamen and caudate nucleus that were indistinguishable from those given by more invasive methods that required metabolite-corrected plasma time–activity curves. However, $B_{max}$ and $K_D$ determined with TEM or with plasma input function methods were associated with larger between-subject variability than binding potential ($BP_{ND}$) as measured with regional SD across subjects: a 26% coefficient of variation (COV) for $B_{max}$ (*6*), compared with typically less than 10% COVs for $BP_{ND}$ (*7*) for age- and sex-similar samples. Furthermore, $B_{max}$ determined with TEM or with plasma input function methods showed larger test–retest variability than $BP_{ND}$ (*4*). The authors ascribed their findings to low signal-to-noise ratio (i.e., due to low counts) of the low-specific-activity (LSA) scans. Another potential contributing factor could be the fact that TEM and other published methods (*5*) used an instant moment when the change in the bound amount becomes zero to obtain the amount of bound nonradioactive ligand and the bound-to-free ratio to calculate $B_{max}$ and $K_D$.

To overcome this concern, a new method was developed using a formula that predicted regional time–activity curves of the PET experiments using the bolus-plus-infusion (B/I) scheme (*8*). The formula has been validated for prediction purposes for several PET ligands including $^{11}$C-raclopride (*9–11*). Here, we extend the formula for the derivation of $BP_{ND}$, $B_{max}$, and $K_D$ for bolus injection PET experiments.

The proposed transformation of bolus injection time–activity curves to hypothetical B/I time–activity curves (heretofore referred to as the bolus-plus-infusion transformation [BPIT]) is expected to generate a prolonged steady state (>30 min) on which variables for Scatchard plots are obtained. Therefore, it was anticipated that the proposed BPIT may improve robustness against PET measurement errors over TEM, although it is yet to be examined.

Although $B_{max}$ and $K_D$ measurements were conventionally limited to whole putamen and caudate nucleus, the recent introduction of functional subdivisions of the striatum, which include 5 motor, affective, and limbic subdivisions per side (*12,13*), is a new focus in dopamine system research with PET. Subsequent studies demonstrated differential involvements of the subdivisions in various neuropsychologic and substance addiction conditions, including schizophrenia (*14,15*), Tourette syndrome (*7*), and alcoholism (*16,17*). Therefore, methods for $B_{max}$ and $K_D$ calculation of dopamine $D_2/D_3$ receptors have to be validated against smaller subdivisions that are expected to be associated with greater PET measurement errors. The primary aim of this study was to examine whether TEM and BPIT are robust when applied to functional striatal subdivisions.

To this end, we examined age-associated changes in $B_{max}$ and $K_D$ in striatal subdivisions. Age-associated decreases in dopamine $D_2/D_3$ receptors have been established in the human brain in vivo with PET (*18,19*) and in postmortem studies (*20,21*). Further, age-associated decreases in $BP_{ND}$ have been reported to differ among striatal subdivisions (*22,23*). Regarding $B_{max}$ and $K_D$, Rinne et al. (*24*) showed an age-related decrease in $B_{max}$ on the whole striatum using TEM. When left and right putamen and caudate nucleus were treated separately, the decrease in $B_{max}$ remained statistically significant in the right putamen only. These findings suggested a possibility that TEM was prone to a lower signal-to-noise ratio in smaller volumes. Therefore, examination of age-related changes in $B_{max}$ and $K_D$ in striatal subdivisions should serve as a challenging test for the utility of TEM and BPIT in smaller volumes of interest (VOIs). It was anticipated that these methods, when validated for functional subdivisions through this study, would provide useful tools for improving our understanding of the roles of dopamine $D_2/D_3$ receptors in normal human functions and in neuropsychiatric disorders.

## MATERIALS AND METHODS

### Theory

Carson et al. (*8*) advanced the following prediction formula for time–activity curves of regions, $A_T(t)$ of B/I experiments using observed time–activity curves, and A(t) of bolus injection scans:

$$A_T(t) = \frac{T_B \times A(t) + \int_0^{\tau} A(u)du}{T_B + T_I}, \qquad \text{Eq. 1}$$

where $T_I$ is the duration of the PET scan (min) and $T_B$ (min) is a time constant, originally denoted by $K_{bol}$ and to be defined for each radioligand. The formula is applicable to time–activity curves in plasma, C(t), of free and bound radioligand in tissue, F(t) and B(T), respectively, and in receptor-free regions, R(t). The original intention of the formula was to obtain a population mean $T_B$ for B/I experiments.

Here, we demonstrate mathematically that the $B_{max}$ and $K_D$ of receptor systems can be obtained by BPIT via 1 pair of high-specific-activity (HSA) and LSA bolus injection PET scans, as conventionally used (*5*). In LSA experiments in which the amount of bound ligand is not negligible, we have the following set of differential equations (*5*):

$$\frac{dA(t)}{dt} = K_1 \times C(t) - k_2 \times F(t)$$
$$\frac{dB(t)}{dt} = f_{ND} \times k_{on} \times (B_{max} - B(t)/SA) \times F(t) - k_{off} \times B(t) \qquad \text{Eq. 2}$$

where $K_1$ and $k_2$ are blood-to-brain and brain-to-blood transport rate constants, respectively; $f_{ND}$ is the tissue-free fraction; SA is the specific activity; and $k_{on}$ and $k_{off}$ are bimolecular association and dissociation rate constants, respectively. $B_{max}$ here denotes the density of receptors that are unoccupied by endogenous ligand and corresponds to $B_{avail}$ proposed by Innis et al. (*25*). Applying Equation 1 to Equation 2 for A(t) and R(t), we obtain:

$$\frac{dA_T(t)}{dt} = K_1 \times C_T(t) - k_2 \times F_T(t)$$
$$\frac{dR_T(t)}{dt} = K_1^R \times C_T(t) - k_2^R \times R_T(t) \qquad \text{Eq. 3}$$

where the subscript T indicates variables after BPIT using Equation 1, and the superscript R denotes variables of the receptor-free region. When $A_T(t)$ of multiple regions, $R_T(t)$, and $C_T(t)$ approach their plateaus ($A_C$, $R_C$, and $C_C$, respectively) after time t* with optimized $T_B$, Equation 3 guarantees that $F_T(t)$ and $B_T(t)$ (i.e., $A_T(t) - F_T(t)$) also approach plateaus ($F_C$ and $B_C$, respectively). For $t > t^*$, the lower portion of Equation 2 is applicable to $F_C$ and $B_C$. After rearrangement and $dB_T(t)/dt = 0$, we obtain the Eadie-Hofstee equation (Eq. 4):

$$\frac{B_C}{SA} = -\frac{K_D}{f_{ND}} \times \frac{B_C}{F_C} + B_{max}. \qquad \text{Eq. 4}$$

In practice, $B_{max}$ and $K_D/f_{ND}$ are determined using available $A_C - R_C$ and $A_C/R_C - 1$ in place of $B_C$ and $B_C/F_C$, respectively, in Equation 4. $F_C$ is in fact equal to $R_C$, assuming negligible regional differences in nondisplaceable distribution volume, $V_{ND}$ (i.e., $K_1/k_2 = K_1^R/k_2^R$) (*25*). $BP_{ND}$ is defined for HSA scans only where $B_C$ is negligible:

$$BP_{ND} = \frac{f_{ND}}{K_D} \times B_{max} = \frac{B_C}{F_C} = \frac{A_C}{R_C} - 1. \qquad \text{Eq. 5}$$

It appears possible to set $T_I$ in BPIT independent of the scan length ($T_S$) for the purpose of data analysis. We theorized that setting $T_I$ and $T_S$ to equal values (i.e., $T_I = T_S$) would yield time-consistent estimates of $B_{max}$ and $K_D$, and that setting $T_I$ and $T_S$ to unequal values would result in systematic biases. If validated, this would demonstrate that BPIT settings for $T_I$ and $T_S$ must be equal as originally predicted by the formula in Equation 1 (*8*).

### Subjects

Eighty-one subjects who underwent HSA and LSA $^{11}$C-raclopride PET scans are included in this analysis. Subjects were participants of 3 ongoing research projects. One project (*26*) comprised patients with restless legs syndrome ($n = 23$; mean age ± SD, 59.3 ± 9.3 y; 13 women and 10 men) and healthy subjects ($n = 32$; mean age ± SD, 59.3 ± 8.2 y; 17 women and 15 men). Inclusion and exclusion criteria for restless legs syndrome subjects are described elsewhere (*26*). Participants of the other 2 projects ($n = 27$; mean age ± SD, 24.2 ± 4.3 y; 14 women and 13 men) were healthy subjects (McCaul and Wand, unpublished data, 2012; (*7*)). Briefly, healthy subjects were without a current or past history of neurologic and psychiatric diseases and substance addiction or dependence and showed no abnormal findings on physical examination at the time of participation. Detailed inclusion and exclusion criteria can be found elsewhere (*7,17,26*). Data of all 81 participants were used for evaluation of analysis methods. All healthy subjects who underwent the 2 scans during the daytime ($n = 47$; age range, 18–77 y; 23 women and 24 men) were included for examination of age-related changes in $BP_{ND}$, $B_{max}$, and $K_D$. Subjects gave signed informed consent before their participation. The consent forms were approved by the institutional review board of the Johns Hopkins University.

### PET and MRI Procedures

*PET Procedures.* PET was performed on an Advance scanner (GE Healthcare) with a 14.875-cm axial field of view. Before the scan, a catheter was placed in the antecubital vein of the participant's left arm for the tracer injection. In selected subjects ($n = 33$), another catheter was inserted in the right radial artery to obtain arterial blood samples. Then, the subject was positioned in the scanner with the head lightly immobilized with a custom-made thermoplastic mask to reduce head movement during the scan. After a transmission scan with a $^{68}$Ge source for attenuation correction, a 90-min emission scan in 3-dimensional mode was started with a slow bolus injection of $^{11}$C-raclopride (714.1 ± 44.4 MBq [19.3 ± 1.2 mCi]). In scans with an arterial catheter, arterial blood was sampled at rapid intervals (<5 s) initially and with prolonging intervals toward the end of the emission scan. Selected samples were analyzed by high-pressure liquid chromatography for radioactive metabolites in plasma using previously reported methods (*27*). $^{11}$C-raclopride was synthesized with minor changes in purification and formulation according to the published procedure (*28*). In LSA scans, nonradioactive raclopride was added to the $^{11}$C-raclopride solution targeting to achieve an SA of 555 MBq (15 mCi)/μmol. The final SA adjusted to the injection time was used for the calculation of $B_{max}$ and $K_D$. Observed SA averaged 383.2 ± 244.2 GBq (10,357.0 ± 6,601.2 mCi)/μmol (range, 60.0–1,330.6 GBq [1,622.8–35,961.0 mCi]/μmol) and 640.1 ± 148 MBq (17.3 ± 4.0 mCi)/μmol (range, 366.3–1,098.9 MBq [9.9–29.7 mCi]/μmol) for HSA and LSA scans, respectively.

Each emission scan was reconstructed to 35 transaxial images of 128 ×128 voxels by a backprojection algorithm using the manufacturer-provided software corrected for attenuation, scatter, and dead time. The resulting resolution was approximately 6 mm in full width at half maximum (*29*).

*MRI Procedures.* On a separate occasion, a spoiled-gradient-sequence MRI scan was obtained for each subject using the following parameters: repetition time, 35 ms; echo time, 6 ms; flip angle, 458; slice thickness, 1.5 mm with no gap; field of view, 24 × 18 cm; and image acquisition matrix, 256 × 192, reformatted to 256 × 256.

### PET Data Analysis

*VOIs.* VOIs for the putamen, caudate nucleus, and cerebellum were defined on the MR image using the 3-dimensional interactive-segmentation mode of a locally developed VOI-defining tool (VOILand) (*30*). Then, striatal VOIs were subdivided to the ventral striatum and anterior and posterior putamen and caudate nucleus (5 subdivisions per side (*13*)) using a semiautomated method (*30*) that incorporated anatomic guidance based on postmortem human materials (*31*). The anterior putamen and anterior and posterior caudate nucleus were classified as associative striatum, whereas the posterior putamen represented motor striatum and the ventral striatum consisted of limbic striatum (*12*). VOIs were transferred from MRI to PET space according to MRI-to-PET coregistration parameters obtained with an SPM5 module for this purpose ((*32*); available at www.fil.ion.ac.uk/spm5) and applied to PET frames to obtain regional time–activity curves.

*Optimization of $T_B$.* First, $T_B$ was optimized by minimizing the sum of the SDs of $A_T(t)$, $R_T(t)$, and $C_T(t)$ across PET frames from t* to 90 min for a t* of 30, 40, and 50 min for each scan for subjects with arterial blood samples. Values of $A_C$, $R_C$, and $C_C$ were obtained as respective means of $A_T(t)$, $R_T(t)$, and $C_T(t)$ between t* and 90 min. To evaluate achievement of plateaus in BPIT quantitatively, normalized residual sums of squares (nRSS) across t*- to 90-min frames were compared between BPIT and the multilinear reference tissue method with 2 parameters (MRTM2 (*33*)). Calculation formulas for nRSS are $\Sigma(A_T(t) - A_C)^2/A_C$ for BPIT and $\Sigma(A(t) - eA(t))^2/A_C$ for MRTM2, where eA(t) stands for model-predicted A(t) given by MRTM2. MRTM2 was applied to LSA scans for this evaluation after confirming small differences in nRSS between HSA and LSA scans, although the biologic significance of estimated parameters are unclear for LSA scans. After confirming that $A_T(t)$, $R_T(t)$, and $C_T(t)$ reached respective plateaus at least at 40 min on visual inspection and by means of nRSS (see the "Results" section), BPIT was applied to all subjects, setting t* at 40 min without including C(t) in the analysis.

*Evaluation of BPIT.* Regional estimates of $BP_{ND}$ were compared between BPIT, MRTM2 (*33*), and reference tissue graphical analysis (RTGA (*34*)) for HSA scans. Then, estimates of $B_{max}$ and $K_D$ were compared among the following conditions: both $T_I$ and $T_S$ set at 80 or 90 min ($T_I = T_S$) and $T_I$ set at 80 or 100 min with $T_S$ fixed at 90 min (i.e., $TI \neq TS$), as explained in the "Theory" section.

After methodologic evaluations, age-associated changes in $B_{max}$ and $K_D$ were examined in functional subdivisions of the striatum using TEM and BPIT.

*Statistical Approaches.* Data were summarized as means and SD. The coefficient of determination ($R^2$) was used to evaluate correlations between methods and approaches. Pearson correlation coefficients ($r$) and $P$ values were reported to evaluate correlations of $B_{ND}$, $B_{max}$, and $K_D$ to age using the Matlab (The MathWorks) function "corr." ANOVA was used to compare methods across regions (2-way ANOVA) using the Matlab function "anova2."

## RESULTS

Plots of $A_T(t)$ and $R_T(t)$ approached respective plateaus by 30 min in all HSA and LSA scans, as shown in Figure 1. In cases with arterial plasma samples, $C_T(t)$ also remained unchanged after 40 min. BPIT showed about 5 times less

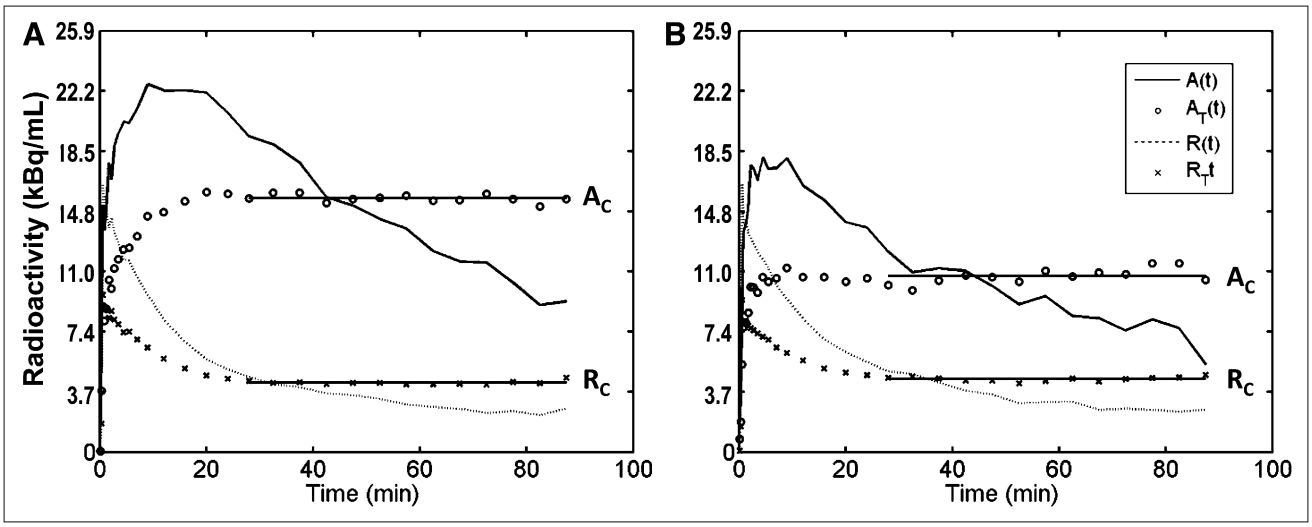


**FIGURE 1.** Observed and transformed regional time–activity curves of anterior putamen, A(t) and $A_T(t)$, respectively, and cerebellum, R(t) and RT(t), respectively, of HSA (A) and LSA (B) $^{11}$C-raclopride scans. Both $A_T(t)$ for all striatal subdivisions and $R_T(t)$ became stable by 30 min in all cases. Assumed plateaus ($A_C$ and $R_C$) are shown by horizontal solid lines.

nRSS than MRTM2 (Table 1) (main effect, $F_1 = 848.78$; $P < 10^{-10}$). Significant region effects were observed ($F_9 = 83.7$; $P < 10^{-10}$), probably because of smaller volumes of posterior caudate nucleus and ventral striatum. For the cases with plasma blood samples, $C_T(t)$ showed nRSS (543.9 ± 318.2 Bq [14.7 ± 8.6 nCi]/mL) that were similar to those of the ventral striatum ($t_{370} = 1.735$; $P > 0.05$) for a t* of 40 min. These findings confirmed that $A_T(t)$, $R_T(t)$, and $C_T(t)$ reached respective plateaus at 40 min and consequently that $F_T(t)$ and then $B_T(t)$ also approached respective plateaus in this time frame. Accordingly, regional $BP_{ND}$ values were identical between the plasma input method (i.e., using $A_T(t)$, $R_T(t)$, and $C_T(t)$ for estimation of $T_B$; $=y$) and the reference tissue method (i.e., using $A_T(t)$ and $R_T(t)$ alone; $=x$) ($y = 1x + 0$; $R^2 = 1.00$; pooling HSA and LSA scan values). Therefore, the remaining analyses were conducted using $A_T(t)$ and $R_T(t)$ alone. The best estimates of $T_B$ averaged at 105 ± 25.8 and 125 ± 30.3 min for HSA and LSA scans, respectively.

For HSA scans, BPIT ($=x$) yielded $BP_{ND}$ values essentially identical to those ofMRTM2 ($=y1$) and RTGA ($=y2$): $y1 = 1.02x - 0.014$, $R^2 = 0.996$, and $y2 = 1.00x - 0.066$, $R^2 = 0.998$. The findings validated BPIT for $BP_{ND}$ for HSA $^{11}$C-raclopride scans. BPIT yielded time-consistent estimates of $B_{max}$ and $K_D$ when both $T_I$ and $T_S$ were set at 80 or 90 min (Table 2). Conversely, BPIT yielded 5% higher or 4% lower values of $B_{max}$ and $K_D$ when $T_I$ was set at 100 min or 80 min for a $T_S$ of 90 min, respectively, than when $T_I$ and $T_S$ were set at 90 min (Table 2). Estimates of $BP_{ND}$ remained unchanged ($R^2 = 1$) when $T_S$ was set at 90 min.

Regional $B_{max}$ and $K_D$ correlated between BPIT and TEM when left and right VOIs were merged (Fig. 2). When compared with BPIT, TEM yielded slightly higher $B_{max}$ and $K_D$ values and suffered some outliers (e.g., $B_{max} >$ 60 pmol/mL; $K_D > 50$ pmol/mL). Correlations were not supported using TEM when left and right sides were treated separately ($R^2 = 0.062$ for $B_{max}$; $R^2 = 0.0012$ for $K_D$), mainly because of an increased number of outliers.

**TABLE 1**
Volumes and nRSS in Functional Striatal Subdivisions

| Parameter | Anterior putamen | Posterior putamen | Anterior caudate nucleus | Posterior caudate nucleus | Ventral striatum |
|---|---|---|---|---|---|
| Volume (mL) | | | | | |
| Left | 1.93 ± 0.29 | 1.88 ± 0.39 | 2.10 ± 0.34 | 0.67 ± 0.20 | 0.87 ± 0.21 |
| Right | 2.00 ± 0.29 | 1.76 ± 0.33 | 2.19 ± 0.33 | 0.66 ± 0.19 | 0.85 ± 0.16 |
| Merged | 3.93 ± 0.53 | 3.65 ± 0.69 | 4.29 ± 0.64 | 1.22 ± 0.37 | 1.72 ± 0.34 |
| nRSS (Bq/mL) | | | | | |
| BPIT | 111 ± 77.7 (3.0 ± 2.1) | 122.1 ± 88.8 (3.3 ± 2.4) | 125.8 ± 99.9 (3.4 ± 2.7) | 477.3 ± 336.7 (12.9 ± 9.1) | 384.8 ± 333 (10.4 ± 9.0) |
| MRTM2 | 558.7 ± 436.6 (15.1 ± 11.8) | 610.5 ± 547.6 (16.5 ± 14.8) | 658.6 ± 577.2 (17.8 ± 15.6) | 2,223.7 ± 1,502.2 (60.1 ± 40.6) | 2,131.2 ± 2,216.3 (57.6 ± 59.9) |

Data are mean ± SD, with nCi/mL in parentheses.

**TABLE 2**
Effects of $T_I$ in Equation 1 and Assumed Scan Length for BPIT ($T_S$) on $B_{max}$ and $K_D$ Estimates

| | | Correlation equations ($R^2$ = coefficient of determination) | |
|---|---|---|---|
| $T_I$ (min) | $T_S$ (min) | $B_{max}$ | $K_D$ |
| 80 | 80 | $y = 1.00x + 0.46$ ($R^2 = 0.989$) | $y = 1.00x + 0.17$ ($R^2 = 0.968$) |
| 80 | 90 | $y = 1.05x - 0.04$ ($R^2 = 1$) | $y = 1.05x - 0.025$ ($R^2 = 1$) |
| 100 | 90 | $y = 0.96x - 0.003$ ($R^2 = 1$) | $y = 0.96x - 0.02$ ($R^2 = 1$) |

$x$= $B_{max}$ or $K_D$ estimates with both $T_I$ and $T_S$ set to 90 min; $y$ = estimates obtained with $T_I$ and $T_S$ set as indicated.

When left and right VOIs were analyzed separately, regional $B_{max}$ decreased as a function of age in 9 of 10 regions (excluding right posterior caudate nucleus) by BPIT, whereas only 4 regions showed correlations by TEM after Bonferroni adjustment (Table 3). When left and right VOIs were combined, BPIT revealed that $B_{max}$ in all 5 subdivisions was inversely correlated with age, whereas TEM failed to identify age-effect in $B_{max}$ posterior caudate nucleus and ventral striatum. BPIT and TEM showed similar rates of decline in $B_{max}$, ranging from 0.47% per year to 0.73% per year in regions. No correlations of $K_D$ with age were observed in any region by BPIT ($0.421 < P < 0.829$, across left and right subdivisions) or by TEM ($0.251 < P < 0.915$). To exemplify these findings, plots of $B_{max}$ against age are shown in Figure 3 for ventral striatum, with left and right VOIs merged.

## DISCUSSION

This study demonstrated that BPIT yielded robust estimates of $B_{max}$ and $K_D$ of dopamine $D_2/D_3$ receptors for functional subdivisions of the striatum using HSA and LSA $^{11}$C-raclopride PET. However, the widely used TEM (*5*), also using the cerebellum as the reference region, showed more unstable estimates when applied to striatal subdivisions than did conventional, larger VOIs for which the method has been validated. Therefore, the current findings support application of BPIT for the newly emerged anatomic demand (*7,12–17*). The improved robustness of BPIT over TEM can be ascribed to the different approaches that the 2 methods assumed to overcome the challenging point (i.e., the equation of dB(t)/dt in Eq. 2) of $B_{max}$ and $K_D$ measurements: Farde et al. (*5*) advanced a solution by focusing on an instant moment when dB(t)/dt became zero in Equation 2. Accordingly, the method was referred to as TEM by Hietala et al. (*4*). In contrast, we devised a simple solution without use of the complicated equation. This study demonstrated that steady-state for BPIT is achieved for $^{11}$C-raclopride scans when t* and $T_I$ were set at 40 and 90 min, respectively. In other words, BPIT uses averages between 40 and 90 min, whereas TEM uses the instant time point. The limited time resolution of PET may be a disadvantageous factor for TEM.

BPIT is a graphical method for model parameter estimation. A close analogy would be RTGA (*34*): the Logan lot of calculated variables, namely $\int A(t)dt/A(T)$ ($=y$) versus $\int R(t)dt/A(T)$ yields $BP_{ND}$ as a slope of the asymptote less 1. RTGA requires an assumed value for $k_2$ of the reference region ($k_2^R$, 0.163 min$^{-1}$ for $^{11}$C-raclopride

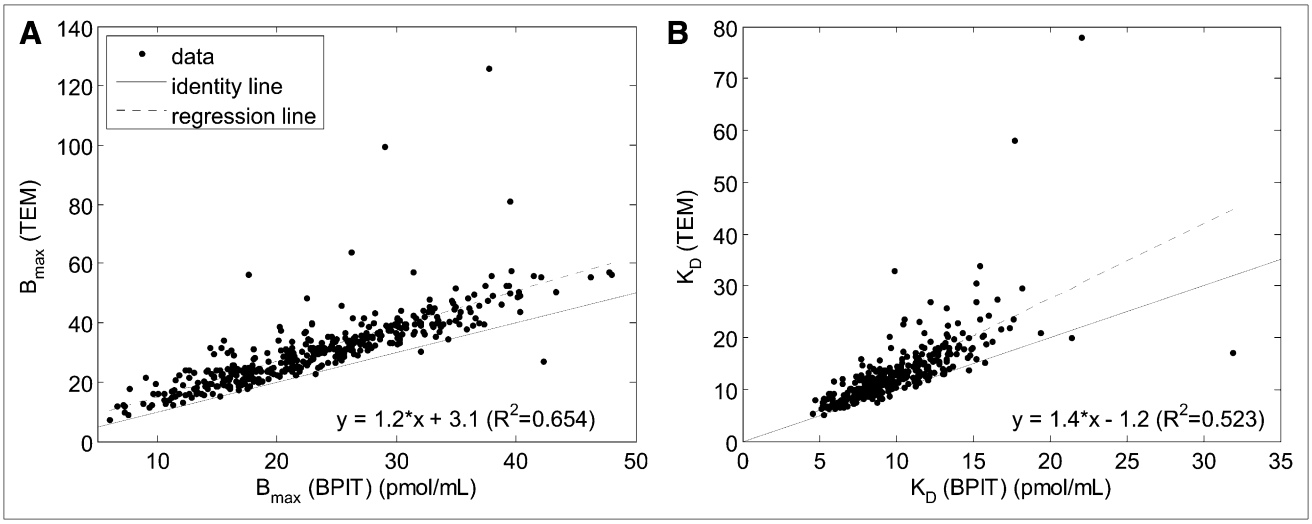


**FIGURE 2.** Scatterplots of regional values of $B_{max}$ (A) and $K_D$ (B), TEM ($=y$) vs. proposed BPIT ($=x$). Data from all subjects ($n$ = 81), 5 subdivisions per subject with left and right VOIs merged, are shown (a total of 405 points). Linear regression equations and coefficients of determination ($R^2$) are shown in each panel.

**TABLE 3**
Correlations of $B_{max}$ to Age in Healthy Subjects

| Striatal subdivisions | Left | | Right | | Merged | |
|---|---|---|---|---|---|---|
| | BPIT | TEM | BPIT | TEM | BPIT | TEM |
| Anterior putamen | | | | | | |
| Pearson correlation coefficient | −0.477 | −0.424 | −0.417 | −0.338 | −0.433 | −0.375 |
| *P* | 0.000701* | 0.00298* | 0.00361* | 0.0201 | 0.00239* | 0.0095* |
| Rates of decline | 0.49% | 0.48% | 0.45% | Not significant | 0.47% | 0.47% |
| Posterior putamen | | | | | | |
| Pearson correlation coefficient | −0.453 | −0.463 | −0.437 | −0.414 | −0.461 | −0.416 |
| *P* | 0.00137* | 0.00105* | 0.00214* | 0.00386* | 0.0011* | 0.00363* |
| Rates of decline | 0.51% | 0.54% | 0.50% | 0.49% | 0.51% | 0.49% |
| Anterior caudate nucleus | | | | | | |
| Pearson correlation coefficient | −0.508 | −0.363 | −0.483 | −0.428 | −0.508 | −0.476 |
| *P* | 0.000268* | 0.0121 | 0.000579* | 0.00267* | 0.000264* | 0.000719* |
| Rates of decline | 0.62% | Not significant | 0.60% | 0.53% | 0.61% | 0.58% |
| Posterior caudate nucleus | | | | | | |
| Pearson correlation coefficient | −0.34 | −0.227 | −0.452 | −0.285 | −0.411 | −0.258 |
| *P* | 0.0196 | 0.126 | 0.00141* | 0.0519 | 0.00407* | 0.0801 |
| Rates of decline | Not significant | Not significant | 0.73% | Not significant | 0.66% | Not significant |
| Ventral striatum | | | | | | |
| Pearson correlation coefficient | −0.415 | −0.0261 | −0.454 | −0.224 | −0.471 | −0.0694 |
| *P* | 0.00377* | 0.862 | 0.00134* | 0.130 | 0.000844* | 0.643 |
| Rates of decline | 0.62% | Not significant | 0.68% | Not significant | 0.67% | Not significant |

*Statistically significant after Bonferroni adjustment.
Rates of decline per year are relative to $B_{max}$ value at 20 y.

(*34*)). Similarly, the BPIT plot (Fig. 1) uses a calculated variable (Eq. 1) as *y* variable and yields $BP_{ND}$ (Eq. 5). BPIT estimates 1 value of $T_B$ for all regions in each experiment. Techniques for estimating a variable that is assumed to be common across regions was also advanced by Wu and Carson (*35*) for $k_2^R$ for the simplified reference region method (*36*) and by Ichise et al. (*33*) for $k_2^R$ in an independent linear solution. BPIT yielded regional values of $BP_{ND}$ that were indistinguishable from established RTGA and MRTM2 for HSA $^{11}$C-raclopride scans. Thus, we concluded that BPIT is validated for HSA $^{11}$C-raclopride scans.

Because of the time-consistent estimates of $B_{max}$ and $K_D$ obtained with equal values of $T_I$ and $T_S$ and systematic biases seen with unequal $T_I$ and $T_S$ (Table 2), we concluded that $T_I$ must be set at $T_S$ in BPIT as it was verified for the prediction purpose (*8*).

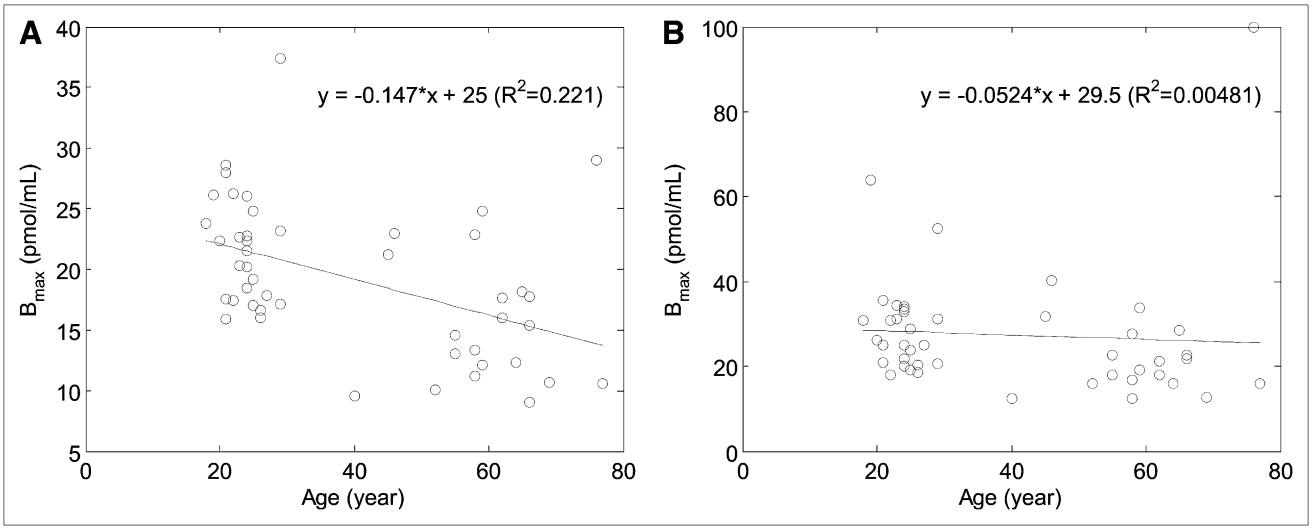


**FIGURE 3.** Scatterplots of $B_{max}$ vs. age for ventral striatum of healthy subjects ($n = 47$) with left and right VOIs merged, given by BPIT (A) and TEM (B). Linear regression equations and coefficients of determination ($R^2$) are shown in each panel.

An age-dependent decline of $BP_{ND}$ of dopamine $D_2/D_3$ receptors has been repeatedly confirmed, predominantly using $^{11}$C-raclopride. To our knowledge, Kim et al. (*23*) was the first to examine age-dependent declines in $BP_{ND}$ in the functional striatal subdivisions. The authors found significant decreases bilaterally in the posterior putamen alone, probably because of the relatively narrow age range and smaller sample size (24–54 y; 13 women and 10 men). This study showed significant decreases in all subdivisions in a population sample, with larger age ranges and larger sample size (18–77 y; 20 women and 22 men). Interestingly, the findings of the 2 studies agreed in that posterior putamen (i.e., motor striatum) showed larger rates of decline than associative striatum and limbic striatum.

Rinne et al. (*24*) reported a rate of decline in $B_{max}$ to be 0.5% per year using $^{11}$C-raclopride, whereas Wong et al. (*37*) reported a rate of 1% per year using an irreversible radioligand $^{11}$C-*N*-methylpiperone and a distinctive analysis method (*38*). Compared with their previous report (*24*), Pohjalainen et al. (*39*) replicated a significant decrease in $B_{max}$ in the right striatum but not in the left striatum, despite a larger number of subjects and inclusion of a wide age range (19–82 y; 21 women and 33 men). Putamen and caudate nucleus were not evaluated independently in this study. The authors did not find any age-associated change in $K_D$, in agreement with earlier reports (*24,37*). To our knowledge, these 3 studies appeared to be the only reports that examined $B_{max}$ and $K_D$ with respect to age in the human brain. Therefore, this study using proposed BPIT is the first to report age-associate decreases of $B_{max}$ in functional striatal subdivisions. Weaker correlations were observed with TEM.

There are several limitations of the study. First, the radioactivity in the vascular volume within a region was omitted from the equations to simplify presentation of the theory (e.g., $A(t) = B(t) + F(t) + v_0 \cdot C(t)$ to be precise, where $v_0$ is the vascular volume). However, because of the linear nature of Equation 1, it is self-evident that the inclusion of $v_0$ does not change the findings. BPIT may suffer degrees of biases in $BP_{ND}$, $B_{max}$, and $K_D$ similar to other established tissue reference methods. Second, observed SA averaged 640.1 MBq (17.3 mCi)/μmol in LSA scans (target SA = 555 MBq [15 mCi]/μmol). The measure was taken to reduce the chances of adverse effects such as akathisia with pharmacologic doses of the dopamine antagonist raclopride (*5*). TEM was validated with significantly lower SA levels (88.8–114.7 MBq [2.4–3.1 mCi]/μmol; (*5*)). Rinne et al. (*24*) also used lower SA levels (92.5–418.1 [2.5–11.3 mCi]/μmol) to examine age-dependent changes in $B_{max}$. In theory, lower SA levels in LSA scans bring LSA points toward the *y*-axis in the Eadie-Hofstee plot (Eq. 4) and contribute to increasing the accuracy of $B_{max}$. Therefore, it should be clarified that the accuracy of TEM estimated in this study cannot be directly compared with these earlier studies. Conversely, BPIT could be applicable to studies even with relatively modest SA in LSA scans.

The most difficult point in the validation of BPIT could be to prove achievement of plateaus. Linear regression may appear appropriate for this purpose. To evaluate achievement of plateaus in an unbiased manner, we used an approach that applies RSS of model fitting. RSS is considered to be composed of errors originating from PET measurement errors and the systematic bias due to disagreement between the model and reality. The results indicated that systematic biases observed with BPIT (i.e., steady increases or decreases of $A_T(t)$, $R_T(t)$, and $C_T(t)$) were significantly lower than systematic biases that were associated with MRTM2, provided PET measurement errors were relatively similar to each other. For this reason, we concluded that plateaus were achieved for PBIT. Further validation may be obtained by actually performing HSA and LSA B/I experiments, as has been reported in animal studies for the opiate receptors (*40*).

## CONCLUSION

This study demonstrated that BPIT is a valid method for measurements of $BP_{ND}$, $B_{max}$, and $K_D$ of dopamine $D_2/D_3$ receptors using $^{11}$C-raclopride PET scans. The method yielded more robust estimates of $B_{max}$ and $K_D$ in smaller striatal subdivisions than the widely used TEM. Age-dependent declines in $B_{max}$ were observed in functional striatal subdivisions, except for the posterior caudate nucleus, using BPIT. Therefore, BPIT may be useful for detecting changes in $B_{max}$ and $K_D$ in small functionally uniform regions in various neuropsychiatric and substance abuse disorders.

## DISCLOSURE STATEMENT

The costs of publication of this article were defrayed in part by the payment of page charges. Therefore, and solely to indicate this fact, this article is hereby marked "advertisement" in accordance with 18 USC section 1734.


## ACKNOWLEDGMENTS

We thank the Johns Hopkins Hospital PET Center and Biomedical Cyclotron staff. This work was supported by PHS grants R01 AA012837, R01 AA010158, PO1 AG21190, R01 NS42857, and R01 MH078175. No other potential conflict of interest relevant to this article was reported.


## REFERENCES


1. Wong DF, Wagner HN, Tune LE, et al. Positron emission tomography reveals elevated D2 dopamine receptors in drug-naive schizophrenics. *Science.* 1986;234:1558–1563.
2. Farde L, Wiesel FA, Stone-Elander S, et al. D2 dopamine receptors in neuroleptic-naive schizophrenic patients: a positron emission tomography study with [11C]raclopride. *Arch Gen Psychiatry.* 1990;47:213–219.
3. Wong DF, Pearlson GD, Tune LE, et al. Quantification of neuroreceptors in the living human brain: iv. effect of aging and elevations of $D_2$-like receptors in schizophrenia and bipolar illness. *J Cereb Blood Flow Metab.* 1997;17:331–342.

4. Hietala J, Någren K, Lehikoinen P, Ruotsalainen U, Syvälahti E. Measurement of striatal D2 dopamine receptor density and affinity with [$^{11}$C]-raclopride in vivo: a test-retest analysis. *J Cereb Blood Flow Metab.* 1999;19:210–217.
5. Farde L, Eriksson L, Blomquist G, Halldin C. Kinetic analysis of central [$^{11}$C] raciopride binding to D2-dopamine receptors studied by PET: a comparison to the equilibrium analysis. *J Cereb Blood Flow Metab.* 1989;9:696–708.
6. Farde L, Hall H, Pauli S, Halldin C. Variability in D2 dopamine receptor density and affinity: a PET study with 11C-raclopride in man. *Synapse.* 1995;20:200–208.
7. Wong DF, Brasić JR, Singer HS, et al. Mechanisms of dopaminergic and serotonergic neurotransmission in Tourette syndrome: clues from an in vivo neurochemistry study with PET. *Neuropsychopharmacology.* 2008;33:1239–1251.
8. Carson RE, Channing MA, Blasberg RG, et al. Comparison of bolus and infusion methods for receptor quantitation: application to [$^{18}$F]cyclofoxy and positron emission tomography. *J Cereb Blood Flow Metab.* 1993;13:24–42.
9. Watabe H, Endres CJ, Breier A, Schmall B, Eckelman WC, Carson RE. Measurement of dopamine release with continuous infusion of [$^{11}$C]raclopride: optimization and signal-to-noise considerations. *J Nucl Med.* 2000;41:522–530.
10. Kimes AS, Chefer SI, Matochik JA, et al. Quantification of nicotinic acetylcholine receptors in the human brain with PET: bolus plus infusion administration of 2-[$^{18}$F]F-A85380. *Neuroimage.* 2008;39:717–727.
11. Burger C, Deschwanden A, Ametamey S, et al. Evaluation of a bolus/infusion protocol for $^{11}$C-ABP688, a PET tracer for mGluR5. *Nucl Med Biol.* 2010;37: 845–851.
12. Mawlawi O, Martinez D, Slifstein M, et al. Imaging human mesolimbic dopamine transmission with positron emission tomography: I. Accuracy and precision of $D_2$ receptor parameter measurements in ventral striatum. *J Cereb Blood Flow Metab.* 2001;21:1034–1057.
13. Martinez D, Slifstein M, Broft A, et al. Imaging human mesolimbic dopamine transmission with positron emission tomography. Part II: amphetamine-induced dopamine release in the functional subdivisions of the striatum. *J Cereb Blood Flow Metab.* 2003;23:285–300.
14. Frankle WG, Narendran R, Huang Y, et al. Serotonin transporter availability in patients with schizophrenia: a positron emission tomography imaging study with [$^{11}$C]DASB. *Biol Psychiatry.* 2005;57:1510–1516.
15. Hirvonen J, van Erp TG, Huttunen J, et al. Striatal dopamine D1 and D2 receptor balance in twins at increased genetic risk for schizophrenia. *Psychiatry Res.* 2006;146:13–20.
16. Martinez D, Gil R, Slifstein M, et al. Alcohol dependence is associated with blunted dopamine transmission in the ventral striatum. *Biol Psychiatry.* 2005;58:779–786.
17. Munro CA, McCaul ME, Oswald LM, et al. Striatal dopamine release and family history of alcoholism. *Alcohol Clin Exp Res.* 2006;30:1143–1151.
18. Wong DF, Broussolle EP, Wand G, et al. In vivo measurement of dopamine receptors in human brain by positron emission tomography. Age and sex differences. *Ann N Y Acad Sci.* 1988;515:203–214.
19. Volkow ND, Wang GJ, Fowler JS, et al. Measuring age-related changes in dopamine D2 receptors with $^{11}$C-raclopride and $^{18}$F-N-methylspiroperidol. *Psychiatry Res.* 1996;67:11–16.
20. Seeman P, Bzowej NH, Guan HC, et al. Human brain dopamine receptors in children and aging adults. *Synapse.* 1987;1:399–404.
21. Rinne JO, Lonnberg P, Marjamaki P. Age-dependent decline in human brain dopamine D1 and D2 receptors. *Brain Res.* 1990;508:349–352.
22. Ishibashi K, Ishii K, Oda K, Kawasaki K, Mizusawa H, Ishiwata K. Regional analysis of age-related decline in dopamine transporters and dopamine D2-like receptors in human striatum. *Synapse.* 2009;63:282–290.
23. Kim JH, Son YD, Kim HK, et al. Effects of age on dopamine D2 receptor availability in striatal subdivisions: a high-resolution positron emission tomography study. *Eur Neuropsychopharmacol*. April 19, 2011 [Epub ahead of print].
24. Rinne JO, Hietala J, Ruotsalainen U, et al. Decrease in human striatal dopamine D2 receptor density with age: a PET study with [$^{11}$C]raclopride. *J Cereb Blood Flow Metab.* 1993;13:310–314.
25. Innis RB, Cunningham VJ, Delforge J, et al. Consensus nomenclature for in vivo imaging of reversibly binding radioligands. *J Cereb Blood Flow Metab.* 2007;27:1533–1539.
26. Earley CJ, Kuwabara H, Wong DF, et al. The dopamine transporter is decreased in the striatum of subjects with restless legs syndrome. *Sleep.* 2011;34:341–347.
27. Hilton J, Yokoi F, Dannals RF, Ravert HT, Szabo Z, Wong DF. Column-switching HPLC for the analysis of plasma in PET imaging studies. *Nucl Med Biol.* 2000;27:627–630.
28. Ehrin E, Farde L, de Paulis T, et al. Preparation of $^{11}$C-labelled raclopride, a new potent dopamine receptor antagonist: preliminary PET studies of cerebral dopamine receptors in the monkey. *Int J Appl Radiat Isot.* 1985;36:269–273.
29. DeGrado TR, Turkington TG, Williams JJ, Stearns CW, Hoffman JM, Coleman RE. Performance characteristics of a whole-body PET scanner. *J Nucl Med.* 1994;35:1398–1406.
30. Oswald LM, Wong DF, McCaul M, et al. Relationships among ventral striatal dopamine release, cortisol secretion, and subjective responses to amphetamine. *Neuropsychopharmacology.* 2005;30:821–832.
31. Baumann B, Danos P, Krell D, et al. Reduced volume of limbic system-affiliated basal ganglia in mood disorders: preliminary data from a postmortem study. *J Neuropsychiatry Clin Neurosci.* 1999;11:71–78.
32. Ashburner J, Friston KJ. Rigid body registration. In: Frackowiak RSJ, Friston KJ, Frith CD, et al., eds. *Human Brain Function.* San Diego, CA: Academic Press; 2003:635–654.
33. Ichise M, Liow JS, Lu JQ, et al. Linearized reference tissue parametric imaging methods: application to [$^{11}$C]DASB positron emission tomography studies of the serotonin transporter in human brain. *J Cereb Blood Flow Metab.* 2003;23:1096–1112.
34. Logan J, Fowler JS, Volkow ND, Wang GJ, Ding YS, Alexoff DL. Distribution volume ratios without blood sampling from graphical analysis of PET data. *J Cereb Blood Flow Metab.* 1996;16:834–840.
35. Wu Y, Carson RE. Noise reduction in the simplified reference tissue model for neuroreceptor functional imaging. *J Cereb Blood Flow Metab.* 2002;22:1440–1452.
36. Lammertsma AA, Hume SP. Simplified reference tissue model for PET receptor studies. *Neuroimage.* 1996;4:153–158.
37. Wong DF, Young D, Wilson PD, Meltzer CC, Gjedde A. Quantification of neuroreceptors in the living human brain: III. D2-like dopamine receptors: theory, validation, and changes during normal aging. *J Cereb Blood Flow Metab.* 1997;17:316–330.
38. Wong DF, Gjedde A, Wagner HN Jr, et al. Quantification of neuroreceptors in living human brain. part II. Inhibition studies of receptor density and affinity. *J Cereb Blood Flow Metab.* 1986;6:147–153.
39. Pohjalainen T, Rinne JO, Någren K, Syvälahti E, Hietala J. Sex differences in the striatal dopamine D2 receptor binding characteristics in vivo. *Am J Psychiatry.* 1998;155:768–773.
40. Kawai R, Carson RE, Dunn B, Newman AH, Rice KC, Blasberg RG. Regional brain measurement of Bmax and KD with the opiate antagonist cyclofoxy: equilibrium studies in the conscious rat. *J Cereb Blood Flow Metab.* 1991; 11:529–544.